HHS Public Access

Author manuscript

Neuroimage. Author manuscript; available in PMC 2016 January 01.

Published in final edited form as:

Neuroimage. 2015 January 1; 104: 452–459. doi:10.1016/j.neuroimage.2014.10.027.

Evaluation of Highly Accelerated Simultaneous Multi-Slice EPI for FMRI

L. Chen[*], **A. Vu**[*], **J. Xu**, **S. Moeller**, **K. Ugurbil**, **E. Yacoub**, and **D.A. Feinberg**
University of California, Berkeley

Advanced MRI Technologies, Sebastopol, CA

CMRR, University of Minnesota, Minneapolis, MN

Abstract

Echo planar imaging (EPI) is the MRI technique that is most widely used for blood oxygen level-dependent (BOLD) functional MRI (fMRI). Recent advances in EPI speed have been made possible with simultaneous multi-slice (SMS) methods which combine acceleration factors *M* from multiband (MB) radiofrequency pulses and *S* from simultaneous image refocusing (SIR) to acquire a total of N=*S* × *M* images in one echo train, providing up to N times speed-up in total acquisition time over conventional EPI. We evaluated accelerations as high as N=48 using different combinations of *S* and *M* which allow for whole brain imaging in as little as 100 ms at 3T with a 32 channel head coil. The various combination of acceleration parameters were evaluated by tSNR as well as BOLD contrast-to-noise ratio (CNR) and information content from checkerboard and movie clips in fMRI experiments. We found that at low acceleration factors (N ≤ 6), setting *S*=1 and varying *M* alone yielded the best results in all evaluation metrics, while at acceleration N=8 the results were mixed using both S=1 and S=2 sequences. At higher acceleration factors (N > 8), using *S*=2 yielded maximal BOLD CNR and information content as measured by classification of movie clip frames. Importantly, we found significantly greater BOLD information content using relatively fast TRs in the range 300 ms - 600 ms compared to a TR of 2 s, suggesting that faster TRs capture more information per unit time in task based fMRI.

Keywords

EPI; multiplexed EPI; multiband; simultaneous multi-slice; SMS; SIR; SER; BOLD; functional imaging; fMRI

Corresponding Author: David A. Feinberg, PhD, MD, Helen Wills Neuroscience Institute, University of California, Berkeley, Berkeley, CA, Advanced MRI Technologies, Sebastopol, CA, David.feinberg@berkeley.edu.
[*]Equal contribution

Introduction

Echo planar imaging (EPI) was first introduced by Mansfield over twenty-five years ago (Mansfield, 1977). It has been most commonly used for blood oxygen level-dependent (BOLD) fMRI due to its high BOLD sensitivity and fast acquisition speed. Conventional EPI can acquire a single image slice in tens of milliseconds by collecting a complete kspace in a single shot. However, to cover the whole brain with adequate spatial resolution (e.g. 3mm isotropic), several excitations are required which takes about 2–3 seconds.

To further speed up the acquisition, partial Fourier (Feinberg et al., 1986), parallel imaging (Griswold et al., 2002; Pruessmann et al., 1999; Sodickson et al., 1999) and other undersampling techniques, like GS-model (Liang et al., 2003) and UNFOLD (Madore et al., 1999), have been used to reduce echo train length and gain many consequent benefits such as reduced image distortion, signal dropout and blurring. However, these techniques are limited by their SNR reductions at higher acceleration factors, the extended TE required for optimal T2* and BOLD contrast, and increased sensitivity to motion. Significant scan time reductions are also limited since contrast preparation time spent on fat saturation, diffusion weighting or arterial spin labeling (ASL) are not shortened by these techniques which only shorten the echo train.

Echo volume imaging (EVI) acquires a 3D k-space in one echo train and reduces scan time by avoiding multiple contrast preparations (Mansfield et al., 1994). The longer acquisition time window of EVI increases image blurring and distortion due to T2* decay; and the requirement to fully encode a 3D volume in such a short time limits the spatial resolution and image quality. To mitigate these problems, multi-slab variants of EVI have been used in fMRI to reduce blurring (Posse et al., 2012) as well as multi-shot 3D EPI of segmented k-space acquisition (Poser et al., 2010) and single-shot 3D GRASE (Feinberg et al., 1995; Poser and Norris, 2009; Song et al., 1994; Zimmermann et al., 2011) have been used for high resolution 3D fMRI at 7T. Sensitivity to motion and physiological noise of these and other pulse sequences depends on differences between single-shot vs segmented acquisitions, duration of echo train, spatial resolution and parallel imaging acquisitions.

Simultaneous multi-slice (SMS) EPI, also called multiband EPI, was first introduced by Nunes (Nunes et al., 2006) for fMRI and subsequently demonstrated at 3T and 7T (Moeller et al., 2010, Feinberg et al., 2010). The variant of SMS-EPI, multiplexed-EPI (M-EPI) achieved additional reduction in EPI scan time (Feinberg et al., 2010) by combining S simultaneous echo refocusing (SIR, SER) (Feinberg et al., 2002; Loenneker et al., 1996; Reese et al., 2009) and M multibanded excitation pulse (Larkman et al., 2001; Moeller et al., 2010) to acquire $N=S \times M$ images in one echo train rather than one image with conventional EPI. M-EPI was shown to bring 3-8 fold scan time reduction to fMRI and increased sensitivity to resting state BOLD activity (Feinberg et al., 2010). Blipped-controlled aliasing (blipped-CAIPI), evolved from CAIPRINHA (Breuer et al., 2005) and the earliest SMS EPI approach (Nunes et al., 2006), shifts the relative positions of simultaneously excited slices without causing voxel tilting to improve slice separation (Setsompop et al., 2012), and allows much higher acceleration factors investigated in this study. Blipped-CAIPI SMS-EPI

slice accelerations up to *M*=12 have been demonstrated (Feinberg and Setsompop, 2013; Xu et al., 2013).

Using M-EPI, the same slice acceleration factor N is achievable with multiple choices of SIR and MB factors, here *S* and *M* factors, respectively. Larger *M* factors rely on parallel imaging for acceleration that has g-factor and SNR penalties. While not having these penalties, *S* requires longer readout periods with penalties of increased distortion and, for SIR slices with longer TEs, increased susceptibility dropout. In order to determine the optimal *S* and *M* composition for different acceleration factors, we evaluated different SMS-EPI and M-EPI acquisitions using tSNR, t-test of checkerboard visual responses and classification of movie clip responses.

Methods

Pulse Sequence

Figure 1 illustrates the multiplexed EPI pulse sequence used in this paper. Figure 1 (left) shows the multibanded RF pulse that is composed of several single band RF pulses with frequency offsets among them. Figure 1 (upper right) shows two multiband RF pulses that run sequentially with a readout gradient between them to shift the echo center which is the core of SIR EPI technique. Gradient blips in the slice direction are added at the same time of the blipped phase-encoding gradients to achieve controlled aliasing according to (Setsompop et al., 2012). This blipped-CAIPI scheme shifts the slices along the PE direction to improve their separation by unaliasing (Setsompop et al., 2012). An example of a FOV/3 shift is illustrated in Figure 1 (lower right).

After data acquisition, each readout was separated into parts depending on the *S* factor, with each part containing an echo at the center. The resulting k-spaces are unaliased into multiple slices using a slice-GRAPPA algorithm (Setsompop et al., 2012) with a kernel size 5x5 generated from the reference single band data and multiband data, implemented in an offline reconstruction program written in C++.

Data Acquisition

The imaging protocol used for human studies was approved by the institutional review board (IRB) at the University of California, Berkeley. Seven subjects were scanned using this IRB approved protocol. Each of the subjects provided informed written consent prior to participating in the research. Multiplexed-EPI (M-EPI) images were acquired using a 32-channel phased array coil on a 3T scanner (Trio, Siemens). The study was composed of 3 experiments: resting with constant TR for tSNR evaluation, checkerboard visual stimulus for BOLD CNR evaluation and movie-clip visual stimulus for BOLD information content evaluation. In all experiments, the order of different *S* and *M* combinations were randomized and counterbalanced to avoid any bias due to habituation.

For the comparison using constant TR, oblique axial images were acquired with TR of 500 ms. Comparison using longer TRs were not used due to constraints on scan time humanly tolerable given the large number of acceleration factors being compared. Furthermore, the shorter TR evaluated here better reflects the typical tSNRs of highly accelerated fMRI

studies. For M factors larger than 4, more than 32 slices were acquired to cover the brain. For M factor less than 4, only the center slices were acquired in order to keep TR at 500 ms. The image parameters were: matrix size=80×80, in-plane resolution=2.5×2.5 mm, slice thickness=3 mm, TE=36 ms (for SIR2, TE2 > = 41 ms, for SIR3, TE2 > = 41 ms and TE3 > = 46 ms depending on the RF pulse duration; where TE2 is the TE of the second SIR slice and TE3 is the TE of the third SIR slice), flip angle=30°, partial Fourier factor=6/8, controlled aliasing shift=FOV/4 (Setsompop et al., 2012; Moeller, 2012), RF pulse duration=5.2 ms (for higher multiband factors, $M > 8$, the pulse is lengthened up to 10 ms due to specific absorption rate (SAR) and peak power limitations), slice-GRAPPA reconstruction kernel size=5 and no in-plane accelerations. The echo train length (ETL) were 36-42 ms, 54-61 ms and 73-79 ms for *S* factor of 1, 2, and 3 respectively, with respective echo spacing of 0.58-0.69 ms, 0.90-1.02 ms and 1.22- 1.33 ms. The minimum echo spacing was slightly increased with higher *M* factor since larger blipped-CAIPI gradient blips were required for closer slice spacing. $S = 1, 2$, and 3 and $M = 1, 2, 4, 6, 8, 10, 12, 14$ and 16 were evaluated.

For the fMRI stimulation with checkerboard experiment, the same parameters were used as in the constant TR comparison except 36 slices were acquired while the TR and flip angle were optimized (see Table 1). For conventional EPI, TR was set to 3000 ms for reference (denoted as "*S*1*M*1"). Subjects fixated while watching a flickering 15 s on, 15 s off, 4 Hz checkerboard pattern 9 times per combination of *S* and *M*.

For the movie experiment, the same parameters as the constant TR comparison were used except the number of slices was 48 and slice thickness was 2.5 mm (for isotropic resolution). The slice thickness for this movie data differed because it was collected as part of a larger study outside the scope of this paper and required isotropic resolution for optimal projection onto cortical surfaces. TR and flip angle were as shown in Table 2. It should be noted that for the same N, the TR achievable for the S=1 case was roughly 15% shorter than the S=2 case listed in Table 2 (e.g. minimum TR = 3333, 1000, 500, 333, and 250 ms for N = 1, 4, 8, 12, and 16 respectively). Subjects fixated while watching a 36 s movie 9 times per combination of *S* and *M* at near minimum TR. The 9 repeats were divided across 3 runs with each run showing the movie clip 3 times back-to-back (no pause between within-run repeats). At the start of each run, the final 10 seconds of the movie clip was shown to ensure BOLD transient effects were the same across each presentation of the 36 s movie clip. Two subjects were removed from analysis due to excessive ghosting artifacts from head/eye motion throughout the session.

Analysis

All fMRI data were motion corrected within individual subjects to scans of the same acceleration and resolution using SPM8 (http://www.fil.ion.ucl.ac.uk/spm/) and MATLAB (The Mathworks) software packages. Subsequent analysis was performed using both standard and in-house MATLAB scripts.

For constant TR comparisons, temporal signal-to-noise ratio (tSNR) per voxel was calculated as the temporal mean divided by the temporal standard deviation of a 25 image

time series. Only the slices with the same TE were used to calculate average tSNR within the brain for each combination of *S* and *M*.

For the checkerboard experiment, an independent two-sample t-test (degrees of freedom, df=16) was performed on the mean BOLD response of each 15-second block of stimulus presentation to generate activation maps. Different accelerations were compared based on the mean t-value and the number of voxels with t-value above 2.9 ($p < 0.01$, uncorrected). The same subject specific ROIs were used to generate the mean t-scores and number of significant voxels. The ROIs were defined as the union of all significantly activated voxels ($t > 2.9$, $p < 0.01$) across all accelerations.

For the movie experiment, leave-one-repeat-out classification using linear discriminant analysis (Cox and Savoy, 2003; Kay and Gallant, 2009) was used to measure the BOLD information content in terms of average number of frames correctly classified. To perform the classification, all but one of the repeats were averaged together to generate the training dataset while the left out repeat was used as the testing dataset. Error bars representing standard error of the mean (SEM) were generated by repeating this procedure 9 times with each time leaving out a different repeat for testing. The number of frames to classify (depending on the acceleration factors compared) was defined as 36 s divided by TR.

Results

Constant TR Comparison

Figure 2 shows one image slice acquired from one subject using M-EPI with different S and M factors with the same TE and TR. As the acceleration factor increases, image quality degrades as expected, especially for total acceleration factors greater than 8.

Figure 3 shows the tSNR comparison of constant TR acquisitions. As the *S* factor and *M* factor increase, tSNR generally decreases, as expected. However, at higher accelerations ($N > 8$), for the same total acceleration factor N, $S=2$ generally has higher tSNR than $S=1$ (Figure 3b). Figure 4 shows the comparison of *S2M4* and *S1M8* with comparable image quality except for increased distortion in S2M4 in frontal lobe from susceptibility artifact.

Checkerboard Experiment

Figure 5 shows typical activation maps with different acquisition parameters. These results are summarized across all subjects in Figure 6 which shows the comparison of the mean t-value and number of voxels above the threshold of 2.9 ($p < 0.01$, uncorrected) within subject specific ROIs. For lower acceleration factors ($N \leq 8$), $S=1$ is comparable with, if not better than $S=2$ in terms of this t-value comparison. However, for higher total acceleration factors ($N > 8$), $S=2$ has higher mean t-value and more voxels above the threshold than $S=1$. This is especially the case for the odd SIR2 slices which have a slightly longer TE (41ms) than the even SIR2 slices (36 ms).

Movie Experiment

Figure 7 shows the classification performance for acceleration factors N=1, 4, 8, 12, and 16 in the movie experiment. Figure 7a shows the number of time points correctly classified

with chance plotted in black. The total numbers of possible time points in the 36 second movie clip were 9, 30, 60, 90, and 120, from the slowest to fastest TRs respectively. At high total accelerations (N > =8), S=2 (red) allows significantly more time-points to be classified than with *M* alone, *S*=1 (blue; $p < 0.05$). For low accelerations (N < 8), *S*=1 performs similar if not better than *S*=2 in terms of classified time-points. Figure 7b shows the percent accuracy. Although percent accuracy decreases with faster TRs, this is expected given that the chance level also decreases. Figure 7c shows classification efficiency (percent accuracy divided by chance level). While efficiency peaks around N=8 for S1, efficiency remains steadily high even up to N=16 for S2.

Discussion

The tSNR analysis performed at constant TR with different acceleration parameters shows that tSNR decreases with higher acceleration factor. For higher total acceleration factors (N > 8), *S*=2 yields higher tSNR than *S*=1 for a given N. However, there was little or no improvement in tSNR with *S*=3. The checkerboard and movie experiments were performed to compare the effect of acceleration parameters *S* and *M* on BOLD contrast and information content, respectively. In terms of t-value, *S*=2 is better than *S*=1 for higher acceleration factors (N > 8) while comparable or worse for lower acceleration factors. To be noted, the results presented here evaluate fMRI responses as function of accelerations in visual areas only. As T2* and T1 vary throughout the brain, future studies are necessary to evaluate regional relaxation and susceptibility effects that may impact optimal *S* and *M*.

In terms of BOLD information content using faster TRs, we found that the maximum number of frames classified using a single trial was achieved using TRs in the range of 300 to 600 ms. This indicates that faster TRs provide more information per unit time in certain task based fMRI studies as has been shown in functional connectivity studies (Feinberg et al., 2010). Although the proportion of frames classified (relative to the total number of frames: 36 s/TR) generally decreased with increasing TR, this is expected since classification becomes more difficult with more frames to choose from. Our results based on the absolute number of frames classified is appropriate given that the number classified are much larger than chance and considering that, for *S*1*M*1, even if 100% of possible frames were classified, that would yield only nine time points classified within the 36 second movie. Furthermore, in terms of classification efficiency (percent classified / percent chance; which is proportional to number of time points classified), we show that highly accelerated TRs with S=2 yields the best classification results.

For higher acceleration factors with S=1, i.e., without SIR, the more similar spatial sensitivity profiles of closer slice spacing with very high MB factors (M > 12) makes the parallel imaging technique incapable of differentiating signals from different slices with much accuracy resulting in high levels of noise and slice cross-talk or leakage (high *g*and *L*-factors (Moeller et al., 2012; Xu et al., 2013)). This limitation is determined by the coil sensitivity profile of the 32 channel head coil used in this study. In the case of *M* > 8, degrading multiband unaliasing performance is the dominant factor in reducing the fMRI performance. By using *S*=2 to achieve high N, the distances between multiband slices is doubled with M factor halved resulting in improved slice separation hence lower *g*- and *L*-

factors. Thus for high N, *S*=2 yields the best tSNR, t-values and BOLD information content per unit time.

Given that SIR introduces slice dependent TEs, in practice, the amount of BOLD contrast available will be slice dependent. In the BOLD t-value and information content evaluations, we limit comparisons to S1 and S2 (only ~5ms RF duration difference in TE across SIR2 slices). However, as we have shown in Figure 6, even with this relatively small TE difference, the odd SIR slices (TE=41 ms) are found to exhibit stronger BOLD contrast than the even SIR slices (TE=36 ms). In practice however, minimizing RF duration combined with motion correction/interpolation of data across runs and/or applying typical smoothing kernels (not used in this work) will all help to minimize this TE difference effect. Future work will investigate the practicality of constant TE (CTE) implementations of SIR (Vu et al., 2012) as well as dynamically alternating the TE of individual SIR slices on a per TR basis.In general we find for lower total acceleration factors, both *S*=1 and *S*=2, the SMS EPI with blipped-CAIPI can unalias the images accurately. In this case, the lengthened echo train of *S*=2 is the dominant factor to affect the fMRI performance which makes *S*=1 the preferable option at lower accelerations. Note for the same total acceleration factor, e.g. *S*2*M*4 and *S*1*M*8, because the readout of *S*=2 is longer than *S*=1 in the comparison, *S*1*M*8 has shorter echo train length than *S*2*M*4. SIR echoes are acquired adjacent to each other, and require the longer read gradient to accommodate more signals without g factor noise penalties. Thus, although we denote total acceleration factor N=*S* × *M*; in practice, *S*2*M*4 has longer minimum TR than *S*1*M*8 by about 15% (depending on spatial resolution) as well as more geometric distortions, susceptibility dropout and voxel blurring, notably the same effects of using higher spatial resolution in SMS-EPI, as discussed above.

By utilizing the ~15% advantage in *S*=1 time efficiency (to further reduce TR, reduce *M*, or increase TE) the N for which *S*=1 is optimal could possibly increase beyond the N=8 reported here. In terms of tSNR, reducing the TR by ~15% while keeping total scan time constant would amount to a ~7% increase in tSNR since SNR is generally proportional to the square root of the number of samples (approximating SNR losses due to T1 relaxation as negligible). While this small improvement in tSNR would not change the N for which *S*=1 is optimal for the tSNR metric presented in Figure 3b, using the time efficiency to instead decrease *M* or increase TE may have a larger effect. From the plots of even (matched TE) slices in Figure 6 comparing BOLD contrast in *S*=1 versus *S*=2, this N may increase to as much as 12 but certainly less than 16. Future studies should investigate the optimal set of acceleration and acquisition parameters (*S*, *M*, TE and TR) for each study specific metrics of interest.

The N for which *S*=2 is optimal may also increase when using a coil with more elements (e.g., 48 or 64 channel coil) together with improved reconstruction algorithms since performance at higher *M* factors may be improved under these conditions (Adriany et al., 2005; Cauley et al., 2014; Feinberg et al., 2010; Keil and Wald, 2013; Wiesinger et al., 2004). However, when the receiver channels are less independent, the SMS technique does not perform as well and a small *M* factor should be used. In-plane undersampling, which also depend on the coil performance and reconstruction algorithm (but not evaluated in this study), could be important in reducing echo train length in higher resolution or S > 1

acquisitions. In practice, in-plane accelerations will also allow for reduction in TRs but less so than *M* accelerations since in-plane acceleration doesn't reduce the number of echo trains with their time requirements for excitation pulses, fat saturation pulses, and possible TE delay for optimal BOLD contrast.

Encoding either SIR or higher spatial resolution in EPI, in general, requires longer echo train lengths (ETL) and larger echo spacing (ES) which has deleterious effects in the presence of short T2*. The larger ES sampling time interval lowers bandwidth on the phase encoded axis of k-space increasing blurring (which could contribute to higher tSNR; but the effect size of which is outside the scope of this study) and distortion most noticeable in brain regions with strong susceptibility gradients near air sinuses. Encoding higher spatial resolution imaging also increases ES and ETL whereas in-plane parallel imaging has a counter effect of reducing both the effective ES and ETL. However, a limitation of using two axes of acceleration (in-plane and slice) is that blipped-CAIPI controlled aliasing is performed on the phase encoded axis as is the aliasing of undersampling with in-plane GRAPPA, hence there becomes an even greater demand placed on the spatial sensitivity profiles of the coil and in turn reduces the maximum achievable *M* factor. In this study we used a moderate resolution of 2.5 mm to 3 mm, typical for many fMRI experiments, and at this resolutions *S*=2 was practical with only modest increases in distortion in exchange for improvement in g and L factors compared to *S*=1.

Although we have not directly assessed the effect of SIR slice cross-talk on the image unaliasing of *M* simultaneous slices, SIR leakage is unchanged with greater *M*. SIR leakage occurs mainly at scalp edges orthogonal to image read axis and is reduced with higher in-plane resolution (Feinberg et al., 2002). Although reduced ES in both S1 and S2 was achieved with ramp sampling, the gradient switching period must accommodate not only the blipped phase encode pulses but also the larger blipped slice gradient pulses used in controlled aliasing, and this lowers signal bandwidth and increases ES further. At the 2.5 mm resolution utilized in these comparisons, a difference is discernible in susceptibility artifact in the frontal lobe (Figure 4) and temporal love (not shown). As for the multiband technique, it is limited by RF peak power and SAR. The use of lower flip angles (Ernst angle) to maximize steady state signal and image SNR partially mitigates these problems. Other techniques have recently been proposed to further mitigate MB pulse related increases in peak power or SAR such as: phase optimization of RF subpulses (Wong, 2012), VERSE (Setsompop et al., 2012) as well as the spatially periodic 'PINS' slice excitation (Koopmans et al., 2012; Norris et al., 2011). These techniques will be important when evaluating and applying multiplexed and multiband sequences at higher field strengths.

Conclusions

SMS-EPI (multiplexed and multiband) was evaluated and compared using different acceleration factors (N), SIR (*S*) and multiband (*M*), with a 32 channel receiver coil at 3T. The comparison showed that higher accelerations lead to higher t-values and BOLD information content. For high accelerations (N > 8), use of *S*=2 can mitigate the increased *g*-factor of *M* acceleration alone as limited by the receiver coil array. Through the high accelerations achievable with S=2, we found significantly greater BOLD information using

TRs in the range of 300 ms to 600 ms. This indicates that faster TRs provide more information per unit time in task based fMRI. The ability to exploit this additional information will depend on the experimental design. Future fMRI studies may therefore differ in design from current studies tailored to the typical 2–3 second TRs of non-accelerated EPI that has been available throughout the last two decades of fMRI research.

Acknowledgements

Work supported in part by National Institutes of Health grants: NIH-Human Connectome Project U54MH091657, R44 NS073417.

References

Adriany G, Van de Moortele PF, Wiesinger F, Moeller S, Strupp JP, Andersen P, Snyder C, Zhang X, Chen W, Pruessmann KP, Boesiger P, Vaughan T, Ugurbil K. Transmit and receive transmission line arrays for 7 Tesla parallel imaging. Magn Reson Med. 2005; 53:434–445. [PubMed: 15678527]

Breuer FA, Blaimer M, Heidemann RM, Mueller MF, Griswold MA, Jakob PM. Controlled aliasing in parallel imaging results in higher acceleration (CAIPIRINHA) for multi-slice imaging. Magn Reson Med. 2005; 53:684–691. [PubMed: 15723404]

Cauley SF, Polimeni JR, Bhat H, Wald L, Setsompop K. Interslice Leakage Artifact Reduction Technique for Simultaneous Multislice Acquisitions. Magn Reson Med. 2014; 72:93–102. [PubMed: 23963964]

Cox DD, Savoy RL. Functional magnetic resonance imaging (fMRI) "brain reading": detecting and classifying distributed patterns of fMRI activity in human visual cortex. Neuroimage. 2003; 19:261–270. [PubMed: 12814577]

Feinberg DA, Hale JD, Watts JC, Kaufman L, Mark A. Halving MR imaging time by conjugation: demonstration at 3.5 kG. Radiology. 1986; 161:527–531. [PubMed: 3763926]

Feinberg DA, Kiefer B, Litt AW. High resolution GRASE MRI of the brain and spine: 512 and 1024 matrix imaging. J Comput Assist Tomogr. 1995; 19:1–7. [PubMed: 7822523]

Feinberg DA, Moeller S, Smith SM, Auerbach E, Ramanna S, Glasser MF, Miller KL, Ugurbil K, Yacoub E. Multiplexed echo planar imaging for sub-second whole brain FMRI and fast diffusion imaging. PLoS One. 2010; 5:e15710. [PubMed: 21187930]

Feinberg DA, Reese TG, Wedeen VJ. Simultaneous echo refocusing in EPI. Magn Reson Med. 2002; 48:1–5. [PubMed: 12111925]

Feinberg DA, Setsompop K. Ultra-fast MRI of the human brain with simultaneous multislice imaging. J Magn Reson. 2013; 229:90–100. [PubMed: 23473893]

Griswold MA, Jakob PM, Heidemann RM, Nittka M, Jellus V, Wang J, Kiefer B, Haase A. Generalized autocalibrating partially parallel acquisitions (GRAPPA). Magn Reson Med. 2002; 47:1202–1210. [PubMed: 12111967]

Kay KN, Gallant JL. I can see what you see. Nat Neurosci. 2009; 12:245. [PubMed: 19238184]

Keil B, Wald LL. Massively parallel MRI detector arrays. J Magn Reson. 2013; 229:75–89. [PubMed: 23453758]

Koopmans PJ, Boyacioglu R, Barth M, Norris DG. Whole brain, high resolution spin-echo resting state fMRI using PINS multiplexing at 7 T. Neuroimage. 2012; 62:1939–1946. [PubMed: 22683385]

Larkman DJ, Hajnal JV, Herlihy AH, Coutts GA, Young IR, Ehnholm G. Use of multicoil arrays for separation of signal from multiple slices simultaneously excited. J Magn Reson Imaging. 2001; 13:313–317. [PubMed: 11169840]

Liang ZP, Madore B, Glover GH, Pelc NJ. Fast algorithms for GS-model-based image reconstruction in data-sharing Fourier imaging. IEEE Trans Med Imaging. 2003; 22:1026–1030. [PubMed: 12906256]

Loenneker T, Hennel F, Hennig J. Multislice interleaved excitation cycles (MUSIC): an efficient gradient-echo technique for functional MRI. Magn Reson Med. 1996; 35:870–874. [PubMed: 8744015]

Madore B, Glover GH, Pelc NJ. Unaliasing by fourier-encoding the overlaps using the temporal dimension (UNFOLD), applied to cardiac imaging and fMRI. Magn Reson Med. 1999; 42:813–828. [PubMed: 10542340]

Mansfield P. Multi-planar image formation using NMR spin echoes. Journal of Physics C: Solid State Physics. 1977; 10:L55.

Mansfield P, Harvey PR, Stehling MK. Echo-volumar imaging. MAGMA Magnetic Resonance Materials in Physics Biology and Medicine. 1994; 2:291.

Moeller, S.; Xu, J.; Auerbach, E.; Yacoub, E.; Ugurbil, K. Signal Leakage(L-Factor) as a Measure for Parallel Imaging Performance Among Simultaneously Multi-Slice (SMS) Excited and Acquired Signals; ISMRM 20th Annual Meeting; 2012. p. 0519

Moeller S, Yacoub E, Olman CA, Auerbach E, Strupp J, Harel N, Ugurbil K. Multiband multislice GE-EPI at 7 tesla, with 16-fold acceleration using partial parallel imaging with application to high spatial and temporal whole-brain fMRI. Magn Reson Med. 2010; 63:1144–1153. [PubMed: 20432285]

Moeller, SX Junqian; Auerbach, Edward J.; Yacoub, Essa; Ugurbil, Kamil. Signal Leakage(L-Factor) as a Measure for Parallel Imaging Performance Among Simultaneously Multi- Slice (SMS) Excited and Acquired Signals. Image Reconstruction. ISMRM, melbourne, australia. 2012

Norris DG, Koopmans PJ, Boyacioglu R, Barth M. Power Independent of Number of Slices (PINS) radiofrequency pulses for low-power simultaneous multislice excitation. Magn Reson Med. 2011; 66:1234–1240. [PubMed: 22009706]

Nunes, RG.; Hajnal, JV.; Golay, X.; Larkman, DJ. Simultaneous slice excitation and reconstruction for single shot EPI; ISMRM 14th Annual Meeting. ISMRM; 2006. p. 293

Poser BA, Koopmans PJ, Witzel T, Wald LL, Barth M. Three dimensional echoplanar imaging at 7 Tesla. Neuroimage. 2010; 51:261–266. [PubMed: 20139009]

Poser BA, Norris DG. 3D single-shot VASO using a Maxwell gradient compensated GRASE sequence. Magn Reson Med. 2009; 62:255–262. [PubMed: 19319900]

Posse S, Ackley E, Mutihac R, Rick J, Shane M, Murray-Krezan C, Zaitsev M, Speck O. Enhancement of temporal resolution and BOLD sensitivity in real-time fMRI using multislab echo-volumar imaging. Neuroimage. 2012; 61:115–130. [PubMed: 22398395]

Pruessmann KP, Weiger M, Scheidegger MB, Boesiger P. SENSE: sensitivity encoding for fast MRI. Magn Reson Med. 1999; 42:952–962. [PubMed: 10542355]

Reese TG, Benner T, Wang R, Feinberg DA, Wedeen VJ. Halving imaging time of whole brain diffusion spectrum imaging and diffusion tractography using simultaneous image refocusing in EPI. J Magn Reson Imaging. 2009; 29:517–522. [PubMed: 19243032]

Setsompop K, Gagoski BA, Polimeni JR, Witzel T, Wedeen VJ, Wald LL. Blipped-controlled aliasing in parallel imaging for simultaneous multislice echo planar imaging with reduced g-factor penalty. Magn Reson Med. 2012; 67:1210–1224. [PubMed: 21858868]

Sodickson DK, Griswold MA, Jakob PM. SMASH imaging. Magn Reson Imaging Clin N Am. 1999; 7:237–254. vii-viii. [PubMed: 10382159]

Song AW, Wong EC, Hyde JS. Echo-volume imaging. Magn Reson Med. 1994; 32:668–671. [PubMed: 7808270]

Vu, AT.; Chang, A.; Chen, L.; Feinberg, D. Simultaneous echo refocused (SIR) EPI with constant TE; ISMRM 20th Annual Meeting; 2012. p. 4155

Wiesinger F, Van de Moortele PF, Adriany G, De Zanche N, Ugurbil K, Pruessmann KP. Parallel imaging performance as a function of field strength--an experimental investigation using electrodynamic scaling. Magn Reson Med. 2004; 52:953–964. [PubMed: 15508167]

Wong, E. Optimized Phase Schedules for Minimizing Peak RF Power in Simultaneous Multi-Slice RF Excitation Pulses; ISMRM 20th Annual Meeting. ISMRM; 2012. p. 2209

Xu J, Moeller S, Auerbach EJ, Strupp J, Smith SM, Feinberg DA, Yacoub E, Ugurbil K. Evaluation of slice accelerations using multiband echo planar imaging at 3 T. Neuroimage. 2013; 83:991–1001. [PubMed: 23899722]

Zimmermann J, Goebel R, De Martino F, van de Moortele PF, Feinberg D, Adriany G, Chaimow D, Shmuel A, Ugurbil K, Yacoub E. Mapping the organization of axis of motion selective features in human area MT using high-field fMRI. PLoS One. 2011; 6:e28716. [PubMed: 22163328]

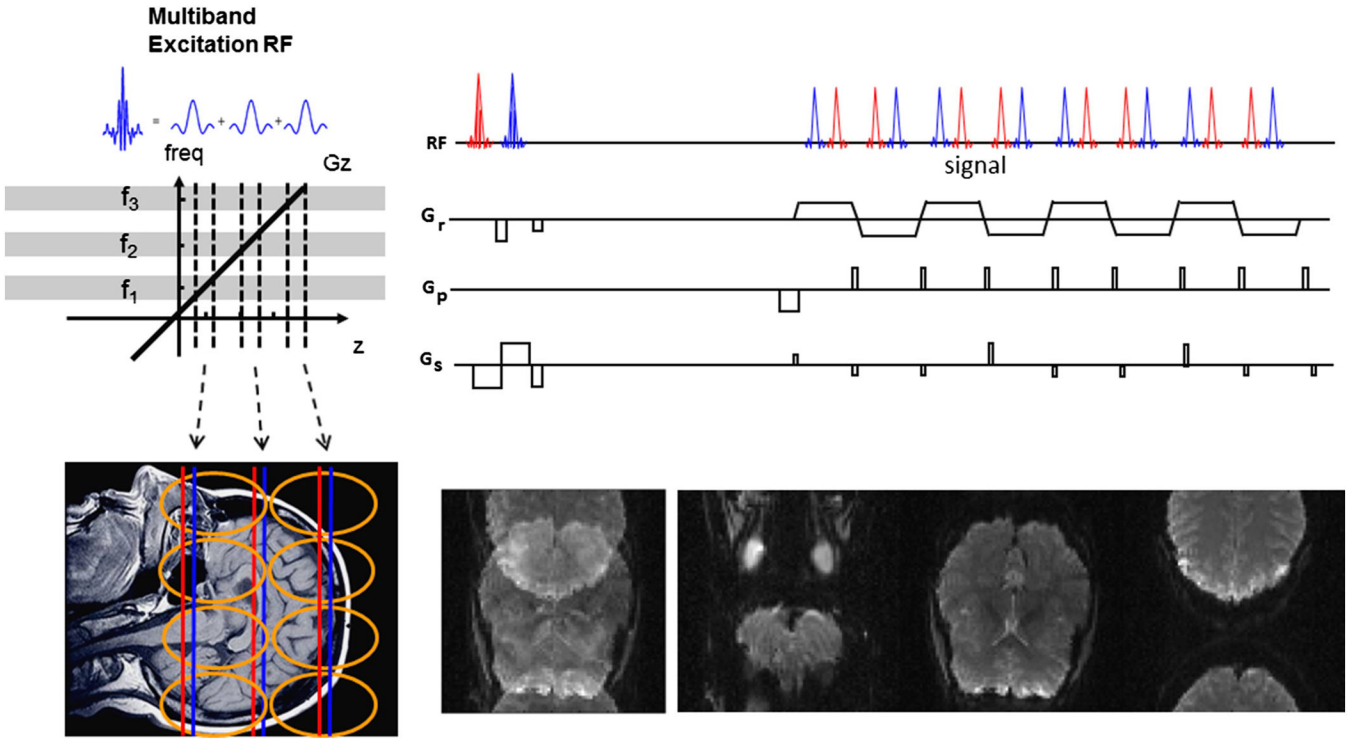

Figure 1.

Multiplexed-EPI pulse sequence illustration. (Left) multiband RF pulse composed of 3 single band RF pulses that have frequency offsets among them. (Upper right) two multiband RF pulses that run sequentially with a readout gradient between them to separate the echoes as in the SIR technique. Extra gradients in the slice direction were added at the same time as the phase-encoding gradient to modulate the phase of multiple slices that were simultaneously excited by the multiband RF to help to separate the slices, as in the blipped controlled aliasing technique. (Lower right) the sum of 3 slices acquired with FOV/3 shift between the slices and the same images separated.

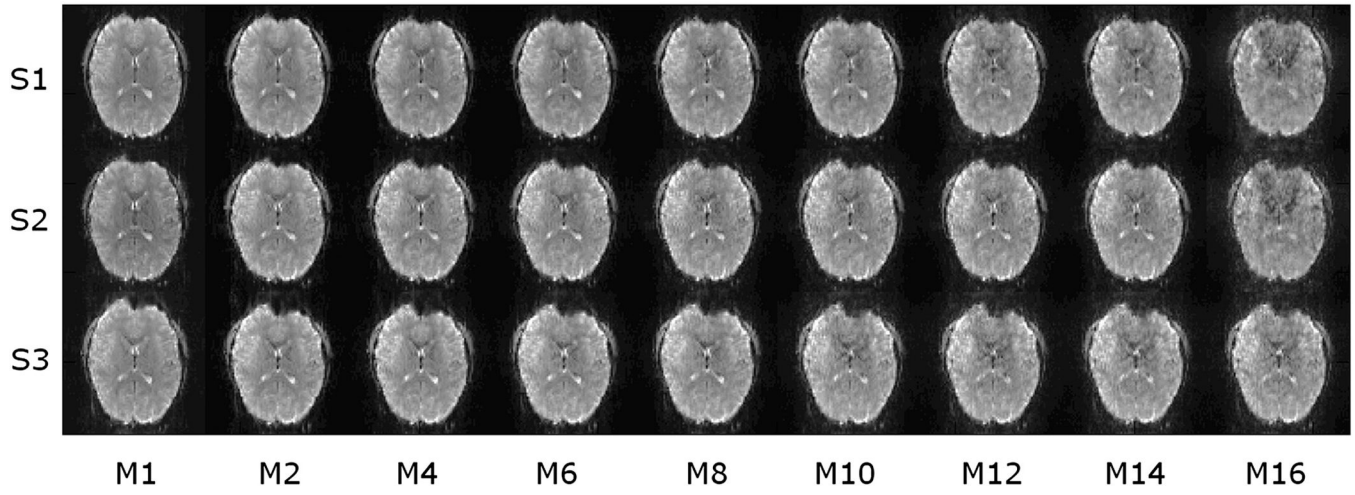

Figure 2.

Representative slices from one subject with multiplexed-EPI using different S and M (SIR and MB) factors at constant TR = 500ms. From top to bottom, S factors are 1, 2 and 3. From left to right, M factors are 1, 2, 4, 6, 8, 10, 12, 14 and 16.

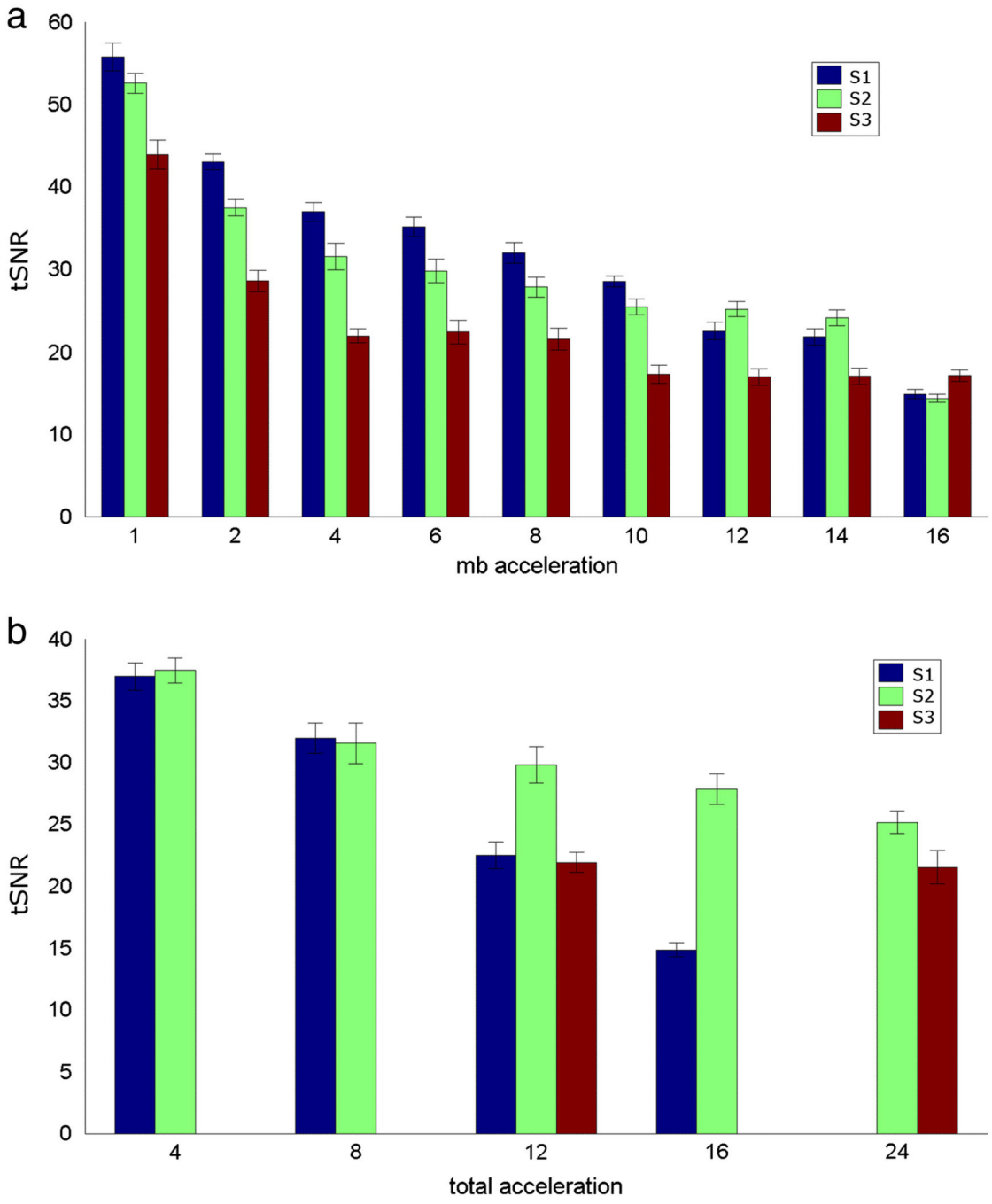

Figure 3.
tSNR comparisons of constant TR acquisitions averaged across subjects. (a) tSNR grouped by multiband factor. (b) tSNR grouped by total slice acceleration factor (N).

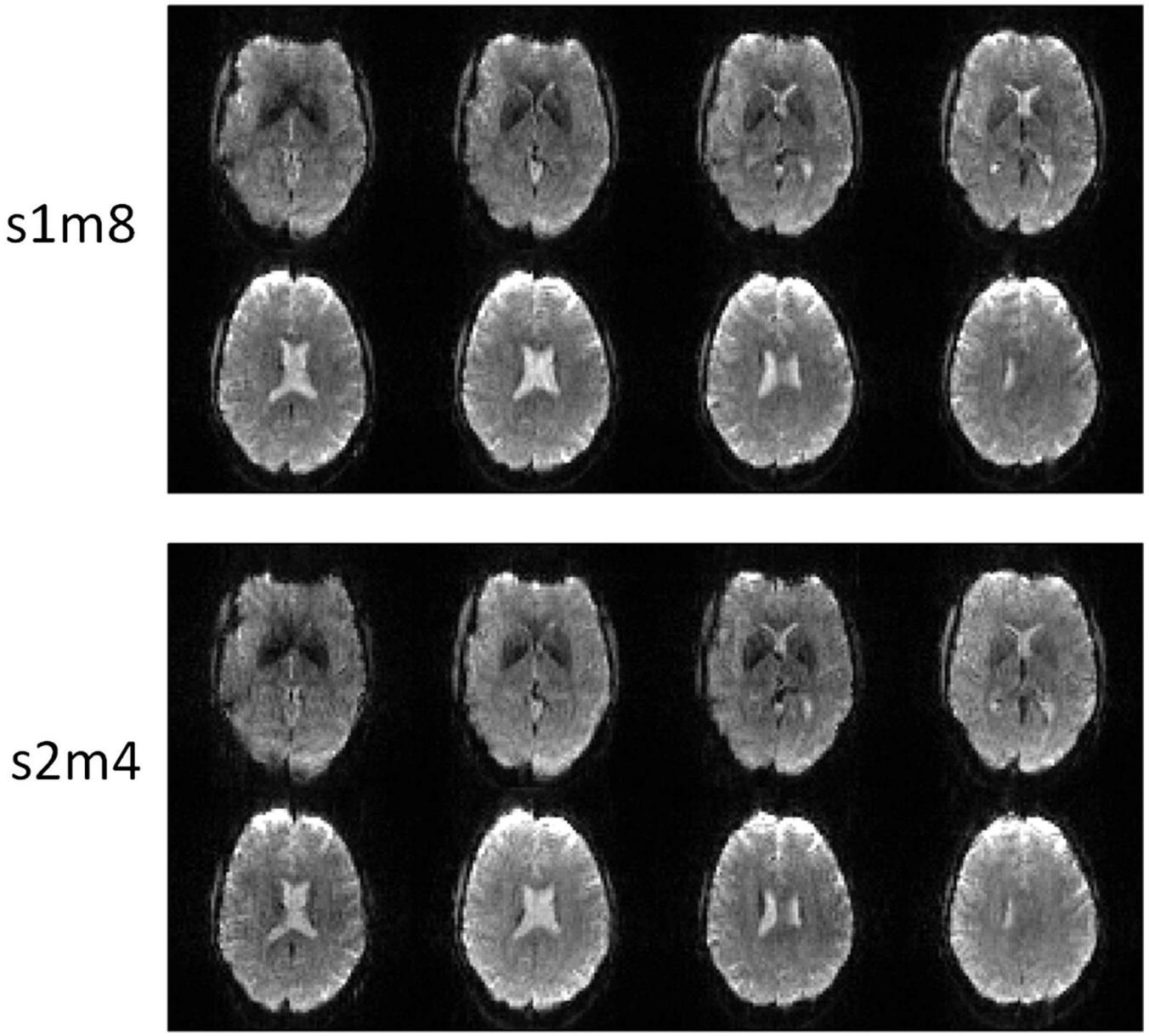

Figure 4.
Image comparison between S2M4 and S1M8. There is similar image quality except for increased distortion in S2M4 in frontal lobe from susceptibility artifact.

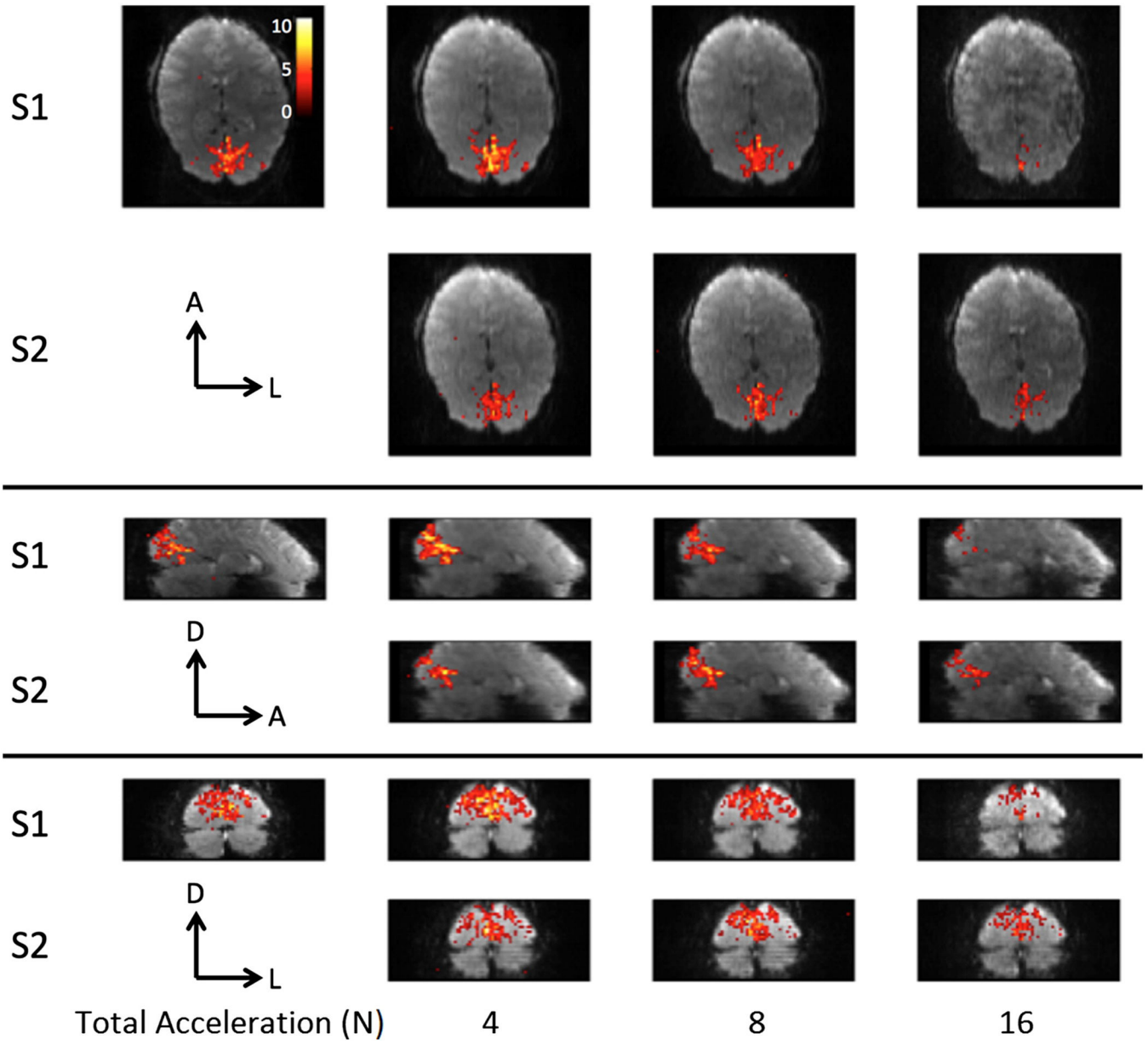

Figure 5.
Representative activation maps from one subject.

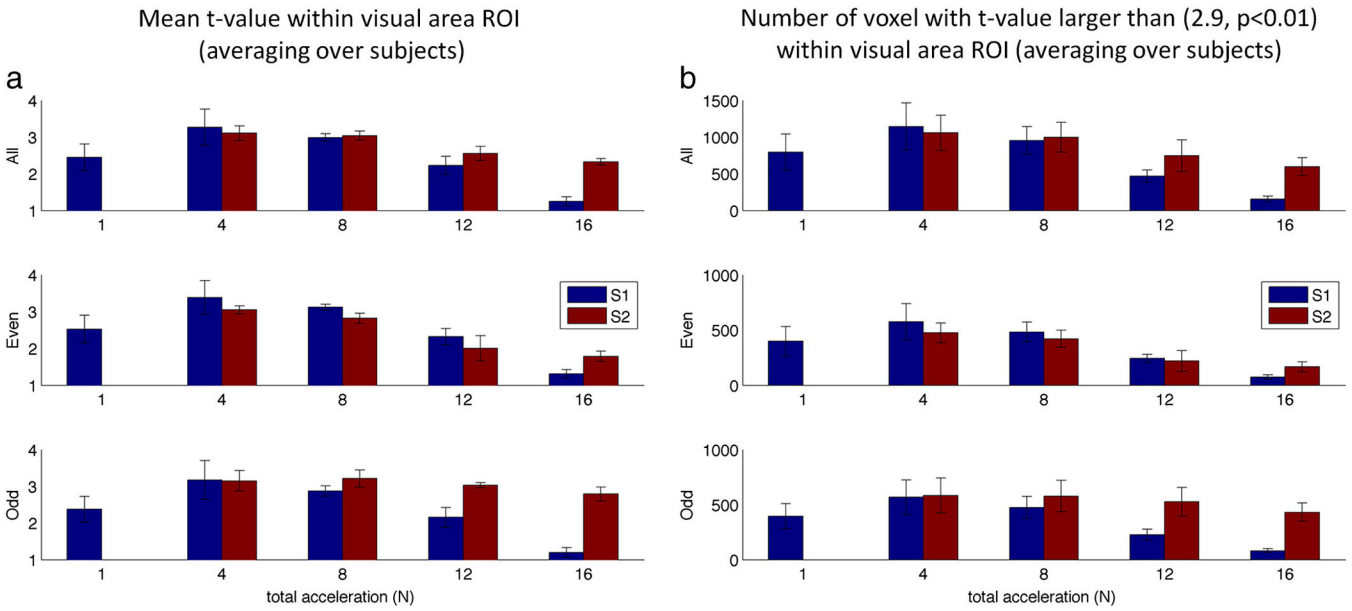

Figure 6.

Mean t-value and number of voxels averaged across subjects in the checkerboard experiment. (a) Mean t-value above the threshold of 2.9 for each acquisition. (b) The number voxels above threshold of 2.9 for each acceleration factor. SIR2 images had two TEs for different slices and the odd slices had longer TE (41 vs 36 ms) that resulted in higher BOLD contrast compared to even slices. Both metrics were calculated within subject specific ROIs.

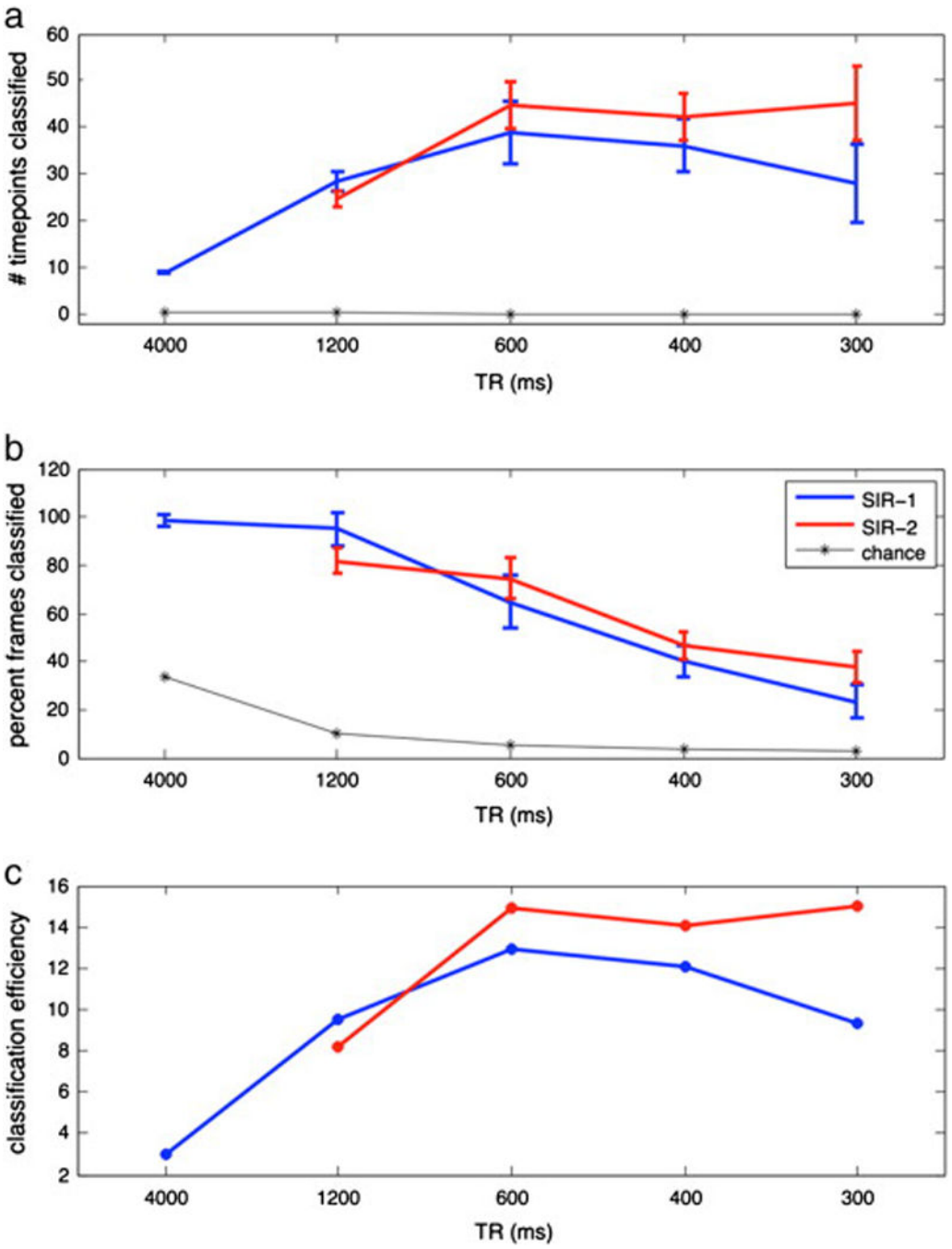

Figure 7.

Classification performance for slice acceleration N = 1 to 16 in the movie experiment. (a) Number of time points correctly classified. The total numbers of possible time points in the 36 second movie clip were 9, 30, 60, 90, and 120, from the slowest to fastest TRs respectively. At high total accelerations (N > =8), *S*=2 allows significantly more time-points to be classified than with MB alone, *S*=1 ($p < 0.05$). For low accelerations (N < 8), *S*=1 performs similar to if not better than *S*=2 in terms of classified time-points. (b) Classification performance in percent accuracy. The percent accuracy goes down with faster TRs as

expected given that the chance level is also going down. (c) Classification efficiency (percent accuracy divided by chance level). While efficiency peaks around N=8 for S1, efficiency remains steadily high even up to N=16 for S2.

Table 1

TR and flip angle values of different acquisitions for the checkerboard experiment. Units (ms, degree) for each combination.

	S1M1	***S2M2***	***S1M4***	***S2M4***	***S1M8***	***S2M6***	***S1M12***	***S2M8***	***S1M16***
TR	3000	1000	750	500	375	*300*	250	250	187.5
FA	80	62	55	47	41	*36*	34	34	30

Table 2

The TR and flip angle values of different acquisitions for the movie experiment. Units are (ms, degree) for each combination.

	S1M1	***S2M2***	***S1M4***	***S2M4***	***S1M8***	***S2M6***	***S1M12***	***S2M8***	***S1M16***
TR	4000	1200	1200	600	600	400	400	300	300
FA	90	67	67	51	51	40	40	36	36